Kinoshita, M., Tobin, H., Ashi, J., Kimura, G., Lallemant, S., Screaton, E.J., Curewitz, D., Masago, H., Moe, K.T., and the Expedition 314/315/316 Scientists
Proceedings of the Integrated Ocean Drilling Program, Volume 314/315/316

Data report: permeability, compressibility, stress state, and grain size of shallow sediments from Sites C0004, C0006, C0007, and C0008 of the Nankai accretionary complex[1]

Brandon Dugan[2] and Hugh Daigle[2]

Chapter contents

[1] Dugan, B., and Daigle, H., 2011. Data report: permeability, compressibility, stress state, and grain size of shallow sediments from Sites C0004, C0006, C0007, and C0008 of the Nankai accretionary complex. *In* Kinoshita, M., Tobin, H., Ashi, J., Kimura, G., Lallemant, S., Screaton, E.J., Curewitz, D., Masago, H., Moe, K.T., and the Expedition 314/315/316 Scientists, *Proc. IODP,* 314/315/316: Washington, DC (Integrated Ocean Drilling Program Management International, Inc.). doi:10.2204/iodp.proc.314315316.208.2011
[2] Department of Earth Sciences, Rice University, Houston TX 77005, USA. Correspondence author: dugan@rice.edu

Abstract

Constant-rate-of-strain consolidation experiments and grain-size analyses are used to characterize the flow and deformation behavior and grain-size distribution of vertically and horizontally oriented specimens from 0 to 100 meters below seafloor at Integrated Ocean Drilling Program Expedition 316 Sites C0004 and C0006–C0008. Interpreted in situ permeability was generally $<10^{-14}$ m^2, but values ranged from 4.6×10^{-14} m^2 to 1.1×10^{-16} m^2 and do not exhibit any definitive trends with depth or grain size. Compression indexes, defining stress-strain behavior during normal consolidation, ranged from 0.15 to 0.9. The overconsolidation ratio (OCR) of vertically oriented specimens, which relates the in situ effective stress to the hydrostatic effective vertical stress, decreased downhole, and most samples had an OCR >1. Grain-size characterization by settling analysis documented that these shallow sediments are dominated by silt and/or clay, with median grain sizes ranging from 0.003 to 0.026 mm, excluding one sand-rich specimen.

Introduction

Integrated Ocean Drilling Program (IODP) Expedition 316 conducted research to understand deformation, fault zone properties, structural partitioning, and fluid flow in the frontal thrust and shallow zone of the megasplay of the Nankai subduction zone (see Screaton et al., 2009). The goals of IODP Expedition 316 fit within the larger objectives of the multiphase Nankai Trough Seismogenic Zone Experiment (NanTroSEIZE) to constrain, monitor, and understand faulting and seismogenesis along megathrusts (Tobin and Kinoshita, 2006).

We focus on the consolidation and flow behavior of shallow sediments, which will be integrated with other shore-based research to understand fluid budgets and deformation of sediments within the Nankai accretionary complex. Whole-round samples were used in constant-rate-of-strain (CRS) consolidation experiments to measure the compression behavior and to estimate the in situ flow properties. Vertically and horizontally oriented specimens from Expedition 316 Sites C0004 and C0006–C0008 were tested to constrain anisotropy of bulk sediment properties in the shallow (<100 meters below seafloor [mbsf]) subsurface (Table T1). We also completed grain-size analysis of geotechnical samples (Table

doi:10.2204/iodp.proc.314315316.208.2011

T1) for comparison with geotechnical properties. Our results complement grain-size, sedimentological, consolidation, and permeability analyses that are ongoing throughout the NanTroSEIZE project. Integrated studies from NanTroSEIZE will provide a full suite of geotechnical and sedimentological parameters to help us understand coupling between flow, deformation, and stability and can be used for inputs into basin-scale models.

Laboratory testing methodology

Whole-round core samples from Sites C0004 and C0006–C0008 (Table T1) were capped and sealed after collection and stored at 4°C to help maintain the natural water content. Samples were taken out of the sealed core liner to conduct CRS consolidation experiments and grain-size analysis following American Society for Testing and Materials (ASTM) International standards (ASTM International 2003; ASTM International, 2006). CRS consolidation experiments are performed at room temperature (20°C) in a rigid confining ring to maintain uniaxial strain. Each specimen was trimmed using a trimming jig, a wire saw, and a sharp-edged spatula to minimize disturbance during preparation and to provide a specimen diameter that was the exact diameter of the rigid confining ring. Once the specimen was in the confining ring, a wire saw, a sharp-edged spatula, and a recess tool were used to shape the specimen into a right cylinder of a fixed height. The use of the trimming jig, confining ring, and recess tool facilitate making specimens of identical diameter and height. Each specimen had an initial height (H_o) of 2.41 cm and an initial diameter of 5.09 cm. A constant, controlled cell pressure (P_c; 386 kPa) is applied to each specimen to ensure saturation. After an initial saturation period of at least 8 h, each specimen is axially deformed at a constant rate of strain. The strain rate ($\dot{\varepsilon}$) was adjusted (ranged from 0.3%–2.0%/h) for each specimen to ensure a pore pressure ratio <0.10 (ASTM International, 2006). The pore pressure ratio depends on the strain rate and the permeability of the specimen. Total axial stress (σ_a), instantaneous sample height (H), and basal pore pressure (P_p) are recorded throughout the experiment. Each experiment is completed at a consolidation stress exceeding the hydrostatic effective vertical stress (σ_{vh}') for the specimen; σ_{vh}' is total vertical stress less hydrostatic fluid pressure. Total vertical stress is determined from bulk density (ρ_b) data (see Expedition 316 Scientists, 2009a, 2009b, 2009c, 2009d). Hydrostatic fluid pressure is calculated assuming a constant seawater density (ρ_w = 1024 kg/m^3).

CRS consolidation experiments provide data to constrain hydraulic conductivity (K) for laboratory conditions and compressibility and to estimate the overconsolidation ratio (Tables T2, T3). Hydraulic conductivity was calculated based on the strain rate and base excess pressure (ASTM International, 2006)

$$K = \dot{\varepsilon} H H_o \gamma_w / 2\Delta u, \quad (1)$$

where

$\dot{\varepsilon}$ = strain rate,
H_o = initial specimen height,
H = instantaneous specimen height,
Δu = base excess pressure, and
γ_w = unit weight of water.

Base excess pore pressure is defined as difference between the basal pore pressure (P_p) and the cell pressure (P_c) ($\Delta u = P_p - P_c$). A smoothed-base excess pore pressure, based on a three-point moving average, is used to calculate hydraulic conductivity. A six-point moving average is used to smooth the strain rate.

We use hydraulic conductivity-void ratio (K-e) data during normal consolidation to define a log-linear relation between K and void ratio for each specimen (Figs. F1, F2) (Lambe and Whitman, 1969). Each specimen-specific model (e.g., Fig. F2) is used to estimate the hydraulic conductivity at the in situ void ratio. We assume that the void ratio at the laboratory-determined preconsolidation stress (e_{pc}') of each specimen represents the in situ void ratio. Initial specimen void ratio was determined in our laboratory from mass and density measurements following the approach presented by Blum (1997). Void ratio during consolidation was determined using the strain data. Hydraulic conductivity is converted to permeability ($k = K\mu/\rho_w g$) using standard seawater density (ρ_w = 1024 kg/m^3), constant dynamic viscosity (μ = 0.001 Pa·s), and the acceleration due to gravity (g = 9.81 m/s^2), which are the laboratory conditions. From the K-e relationship, in situ void ratio, and relation between hydraulic conductivity and permeability, we define the in situ permeability at the in situ void ratio ($k_{e_{pc}'}$) for each specimen (Table T3).

The coefficient of consolidation (c_v), describing coupled deformation and fluid flow, is calculated from the hydraulic conductivity and deformation data using the coefficient of volume compressibility (m_v) (ASTM International, 2006; Craig, 1992),

$$c_v = K/m_v\rho_w g. \quad (2)$$

Stress-strain data during normal consolidation are used to define the compression index (c_c) (Craig, 1992),

$$c_c = (e_{\sigma_a'} - e_{\sigma_a' + \Delta\sigma_a'})/\log[(\sigma_a' - \Delta\sigma_a')/\sigma_a']. \quad (3)$$

The compression index quantifies the relationship between void ratio and vertical effective stress during normal consolidation (Fig. F1; Table T3).

The preconsolidation stress (σ_{pc}') for each vertically oriented specimen is estimated using the work-stress method (Becker et al., 1987). The preconsolidation stress represents an estimate of the maximum effective stress a specimen has experienced. To determine σ_{pc}', we extrapolate the linear portions of the preyield and postyield behavior (Fig. F3). The intersection of the extrapolations defines σ_{pc}' (Becker et al., 1987). We use the preconsolidation stress and the hydrostatic effective vertical stress to define the overconsolidation ratio (OCR) for each vertically oriented specimen (OCR = $\sigma_{pc}'/\sigma_{vh}'$) (Table T3). We use the void ratio at the preconsolidation stress to estimate the in situ void ratio (e_{pc}') (Table T3). An OCR <1 suggests in situ overpressure, an OCR = 1 suggests the sample is at its maximum past effective stress with hydrostatic fluid pressure, and an OCR >1 suggests unloading. Sample disturbance can produce consolidation data with poorly defined σ_{pc}' (Santagata and Germaine, 2002). Saffer (2003) and Dugan and Germaine (2008) present methods to estimate error on interpreted preconsolidation stresses.

To complement the geotechnical data, we also characterized the grain-size distribution for the vertically oriented specimens (Tables T1, T3). All grain-size analyses followed the ASTM standard for particle-size analysis (ASTM International, 2003). No particles were retained by the 2 mm sieve, so the distribution of particles was determined by settling analysis using a hydrometer. To determine the distributions, air-dried specimens are mixed with distilled water and sodium hexametaphosphate, a dispersing agent. The solution is mechanically stirred to create a dispersed suspension, which is transferred into a glass sedimentation cylinder. Regular hydrometer and water temperature readings of the solution are made as the particles settle from suspension. At the end of sedimentation analysis, the contents of the sedimentation cylinder are dried and total particle mass is determined. All data are processed following the ASTM standard and corrected for temperature effects (ASTM International, 2003). The settling analyses are used to define the D_{50} (median particle diameter), D_{25} (particle diameter at which 25% of particles are smaller by mass), and D_{75} (particle diameter at which 75% of particles are smaller by mass) particle diameters and the percentages of sand (>62.5 µm), silt (2–62.5 µm), and clay (<2 µm) (Table T3).

Experimental results

All consolidation and grain-size data are summarized in Table T3. All nomenclature is provided in Table T4. Complete experimental data are provided in 316_CONSOL in "Supplementary material."

Based on interpretation of CRS consolidation experiments, we define the range of geotechnical parameters at Sites C0004 and C0006–C0008. Our estimates of in situ permeability ($k_{e_{pc}'}$) range from 4.6×10^{-14} m^2 to 1.1×10^{-16} m^2 with most permeabilities $<10^{-14}$ m^2 (Table T3; Fig. F4). The compression indexes of the specimens vary widely from a minimum of 0.15 to a maximum of 0.9 (Table T3; Fig. F4). The permeability and compression behavior do not have any strong depth, stress, or sample-orientation trends. The overconsolidation ratio, however, decreases with increasing depth (Fig. F4). The maximum OCR is 42 at 2.39 meters below seafloor (mbsf) (Hole C0006E) and the minimum is <1 at 48.31 and 91.74 mbsf (Holes C0006E and C0007C, respectively) (Table T3).

Grain-size analysis data for Sites C0004 and C0006–C0008 show that the samples are dominated by silt- and clay-sized particles (Table T3). Silt-sized particle contents of the vertically oriented specimens range from 47% to 69%. The highest sand-sized particle content is 44% (48.31 mbsf in Hole C0006E) and the highest clay-sized particle content is 42% (17.31 mbsf in Hole C0004C). Excluding the sand-dominated specimen (48.31 mbsf in Hole C0006E), the median grain size (D_{50}) of specimens ranges from 0.003 to 0.026 mm (Table T3; Fig. F4).

Summary

We used CRS consolidation experiments and grain-size analyses to define the bulk geotechnical properties and grain-size distribution of specimens from 0 to 100 mbsf at Sites C0004 and C0006–C0008, which were drilled and sampled during Expedition 316. Interpreted in situ permeability is generally $<10^{-14}$ m^2 and does not exhibit depth or grain-size trends. Compression indexes range from 0.15 to 0.9 and also do not show any strong trends. The overconsolidation ratio decreases downhole, and most samples had an OCR >1. Grain-size distributions documented that the shallow sections of these sites are domi-

nated by silt- and/or clay-sized particles with median grain sizes ranging from 0.003 to 0.026 mm, with the exception of one sand-rich specimen.

Acknowledgments

This work would not have been possible without the efforts and support of the participants and technical staff of IODP Expedition 316. This research used samples and data provided by the Integrated Ocean Drilling Program (IODP).

References

ASTM International, 2003. Standard test method for particle-size analysis of soils (Standard D422-63[2002]). In *Annual Book of ASTM Standards* (Vol. 04.08): *Soil and Rock* (I): West Conshohocken, PA (Am. Soc. Testing Mater.), 10–17.

ASTM International, 2006. Standard test method for one-dimensional consolidation properties of saturated cohesive soils using controlled-strain loading (Standard D4186-06). In *Annual Book of ASTM Standards* (Vol. 04.08): *Soil and Rock* (I): West Conshohocken, PA (Am. Soc. Testing Mater.)

Becker, D.E., Crooks, J.H.A., Been, K., and Jeffries, M.G., 1987. Work as a criterion for determining in situ and yield stresses in clays. *Can. Geotech. J.,* 24(4):549–564. **doi:10.1139/t87-070**

Blum, P., 1997. Physical properties handbook: a guide to the shipboard measurement of physical properties of deep-sea cores. *ODP Tech. Note,* 26. **doi:10.2973/odp.tn.26.1997**

Craig, R.F., 1992. *Soil Mechanics* (5th ed.): London (Chapman and Hall).

Dugan, B., and Germain, J.T., 2008. Near-seafloor overpressure in the deepwater Mississippi Canyon, northern Gulf of Mexico. *Geophys. Res. Lett.,* 35(2):L02304. **doi:10.1029/2007GL032275**

Expedition 316 Scientists, 2009a. Expedition 316 Site C0004. *In* Kinoshita, M., Tobin, H., Ashi, J., Kimura, G., Lallemant, S., Screaton, E.J., Curewitz, D., Masago, H., Moe, K.T., and the Expedition 314/315/316 Scientists, *Proc. IODP,* 314/315/316: Washington, DC (Integrated Ocean Drilling Program Management International, Inc.). **doi:10.2204/iodp.proc.314315316.133.2009**

Expedition 316 Scientists, 2009b. Expedition 316 Site C0006. *In* Kinoshita, M., Tobin, H., Ashi, J., Kimura, G., Lallemant, S., Screaton, E.J., Curewitz, D., Masago, H., Moe, K.T., and the Expedition 314/315/316 Scientists, *Proc. IODP,* 314/315/316: Washington, DC (Integrated Ocean Drilling Program Management International, Inc.). **doi:10.2204/iodp.proc.314315316.134.2009**

Expedition 316 Scientists, 2009c. Expedition 316 Site C0007. *In* Kinoshita, M., Tobin, H., Ashi, J., Kimura, G., Lallemant, S., Screaton, E.J., Curewitz, D., Masago, H., Moe, K.T., and the Expedition 314/315/316 Scientists, *Proc. IODP,* 314/315/316: Washington, DC (Integrated Ocean Drilling Program Management International, Inc.). **doi:10.2204/iodp.proc.314315316.135.2009**

Expedition 316 Scientists, 2009d. Expedition 316 Site C0008. *In* Kinoshita, M., Tobin, H., Ashi, J., Kimura, G., Lallemant, S., Screaton, E.J., Curewitz, D., Masago, H., Moe, K.T., and the Expedition 314/315/316 Scientists, *Proc. IODP,* 314/315/316: Washington, DC (Integrated Ocean Drilling Program Management International, Inc.). **doi:10.2204/iodp.proc.314315316.136.2009**

Lambe, T.W., and Whitman, R.V., 1969. *Soil Mechanics:* New York (Wiley).

Saffer, D.M., 2003. Pore pressure development and progressive dewatering in underthrust sediments at the Costa Rican subduction margin: comparison with northern Barbados and Nankai. *J. Geophys. Res., [Solid Earth],* 108(B5):2261–2276. **doi:10.1029/2002JB001787**

Santagata, M.C., and Germaine, J.T., 2002. Sampling disturbance effects in normally consolidated clays. *J. Geotech. Geoenviron. Eng.,* 128(12):997–1006. **doi:10.1061/(ASCE)1090-0241(2002)128:12(997)**

Screaton, E.J., Kimura, G., Curewitz, D., and the Expedition 316 Scientists, 2009. Expedition 316 summary. *In* Kinoshita, M., Tobin, H., Ashi, J., Kimura, G., Lallemant, S., Screaton, E.J., Curewitz, D., Masago, H., Moe, K.T., and the Expedition 314/315/316 Scientists, *Proc. IODP,* 314/315/316: Washington, DC (Integrated Ocean Drilling Program Management International, Inc.). **doi:10.2204/iodp.proc.314315316.131.2009**

Tobin, H.J., and Kinoshita, M., 2006. NanTroSEIZE: the IODP Nankai Trough Seismogenic Zone Experiment. *Sci. Drill.,* 2:23–27. **doi:10.2204/iodp.sd.2.06.2006**

Initial receipt: 6 October 2010
Acceptance: 25 March 2011
Publication: 22 June 2011
MS 314315316-208

Figure F1. Constant-rate-of-strain (CRS) consolidation experiment data from Experiment CRS036 (Table T1). Blue circles are the entire data set; green circles are interpreted normal consolidation data that are used for hydraulic conductivity (Fig. F2), compression index (Equation 3), and preconsolidation stress (Fig. F3) analysis. Solid black line is the best-fit model to the normal consolidation data to define the compression index. Complete data for all CRS consolidation experiments are available in 316_CONSOL in **"Supplementary material."**

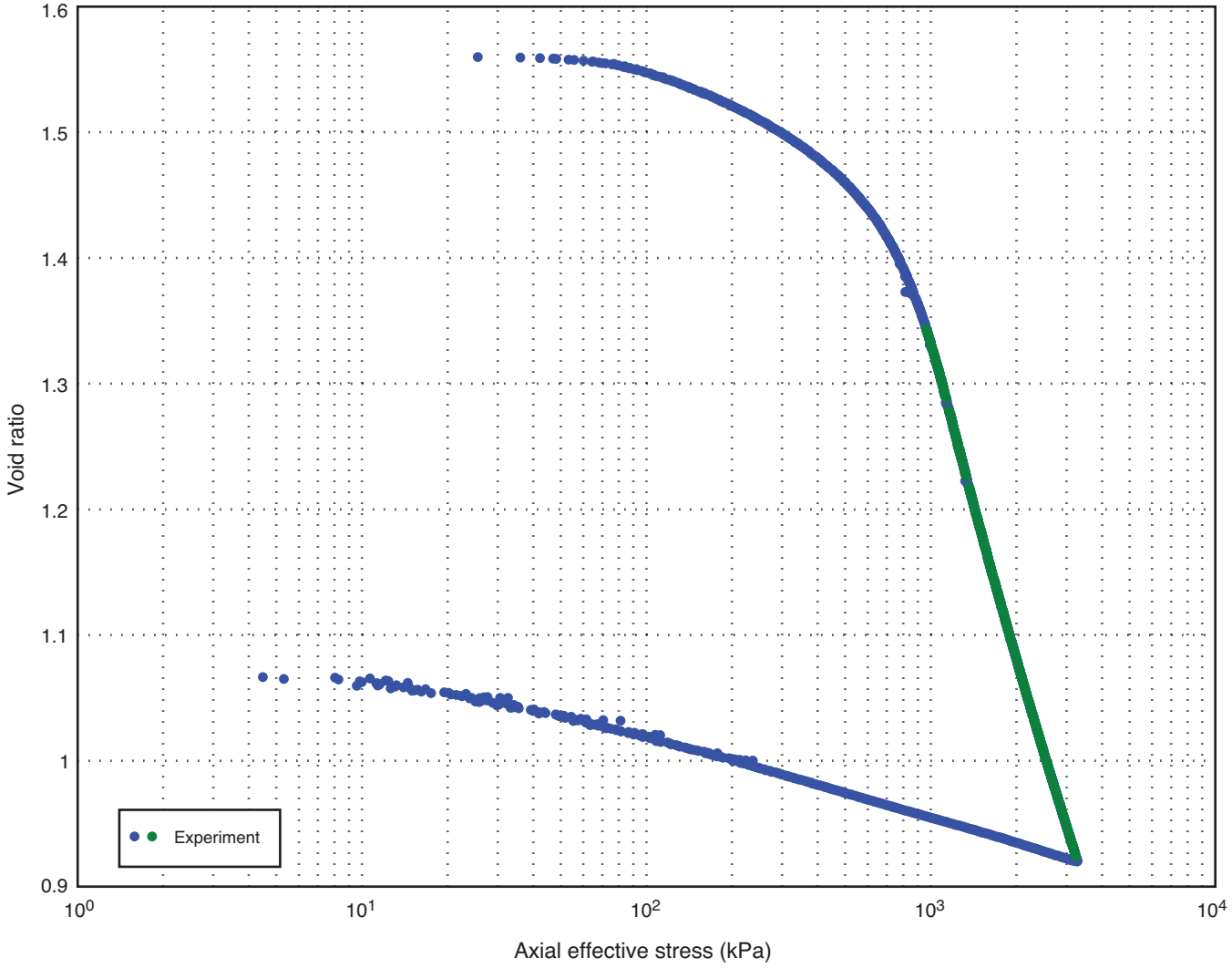

Figure F2. Logarithm of hydraulic conductivity (Equation 1) plotted as a function of void ratio. Data shown are the normal consolidation data from Figure F1 (green circles). Black line is best-fit model to the hydraulic conductivity-void ratio data assuming a log-linear relationship (Lambe and Whitman, 1969). Example is from Experiment CRS036 (Table T1). Complete data for all CRS consolidation experiments are available in 316_CONSOL in **"Supplementary material."**

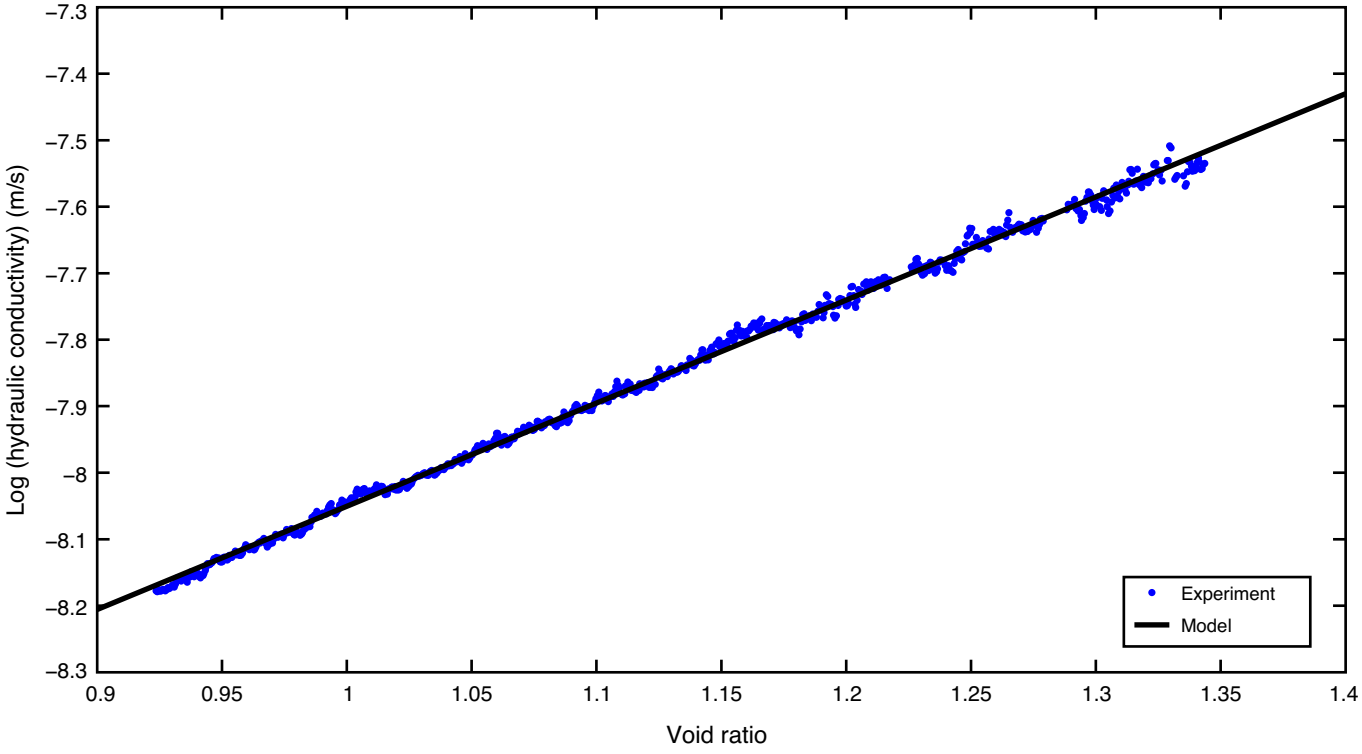

Figure F3. Work-stress analysis (Becker et al., 1987) of experiment CRS036 (Table T1). Red circles are interpreted normal consolidation data, green circles are early time, low-strain data, and blue circles are the entire data set. Solid black lines are best-fit models to the normal consolidation and early time data. Intersection of the best-fit models defines the preconsolidation stress (σ_{pc}') (Becker et al., 1987). Complete data for all CRS consolidation experiments are available in 316_CONSOL in **"Supplementary material."**

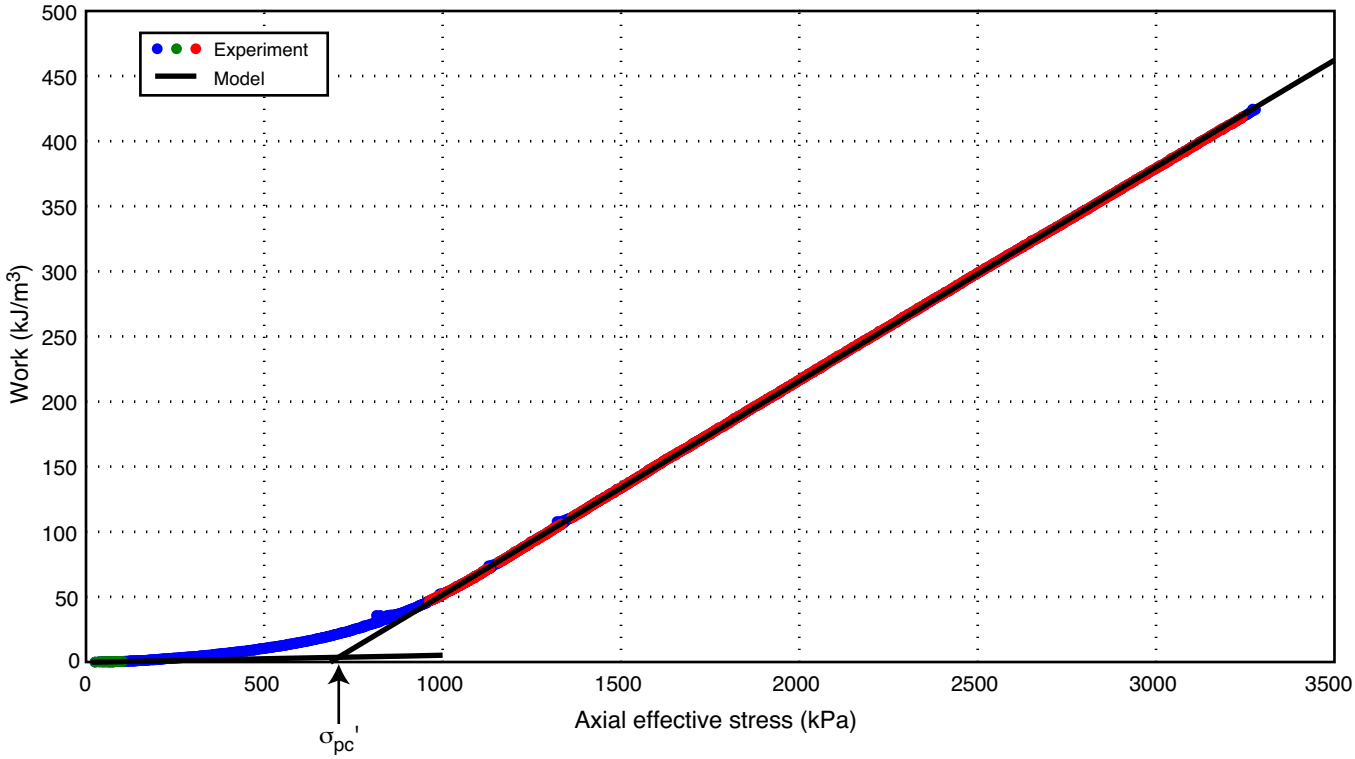

Figure F4. Interpreted geotechnical properties and grain size of specimens from Sites C0004 and C0006–C0008. Solid symbols indicate vertically oriented specimens and open symbols indicate horizontally oriented specimens. **A.** In situ permeability (k). **B.** Compression index (c_c). **C.** Overconsolidation ratio. **D.** Median grain size (D_{50}).

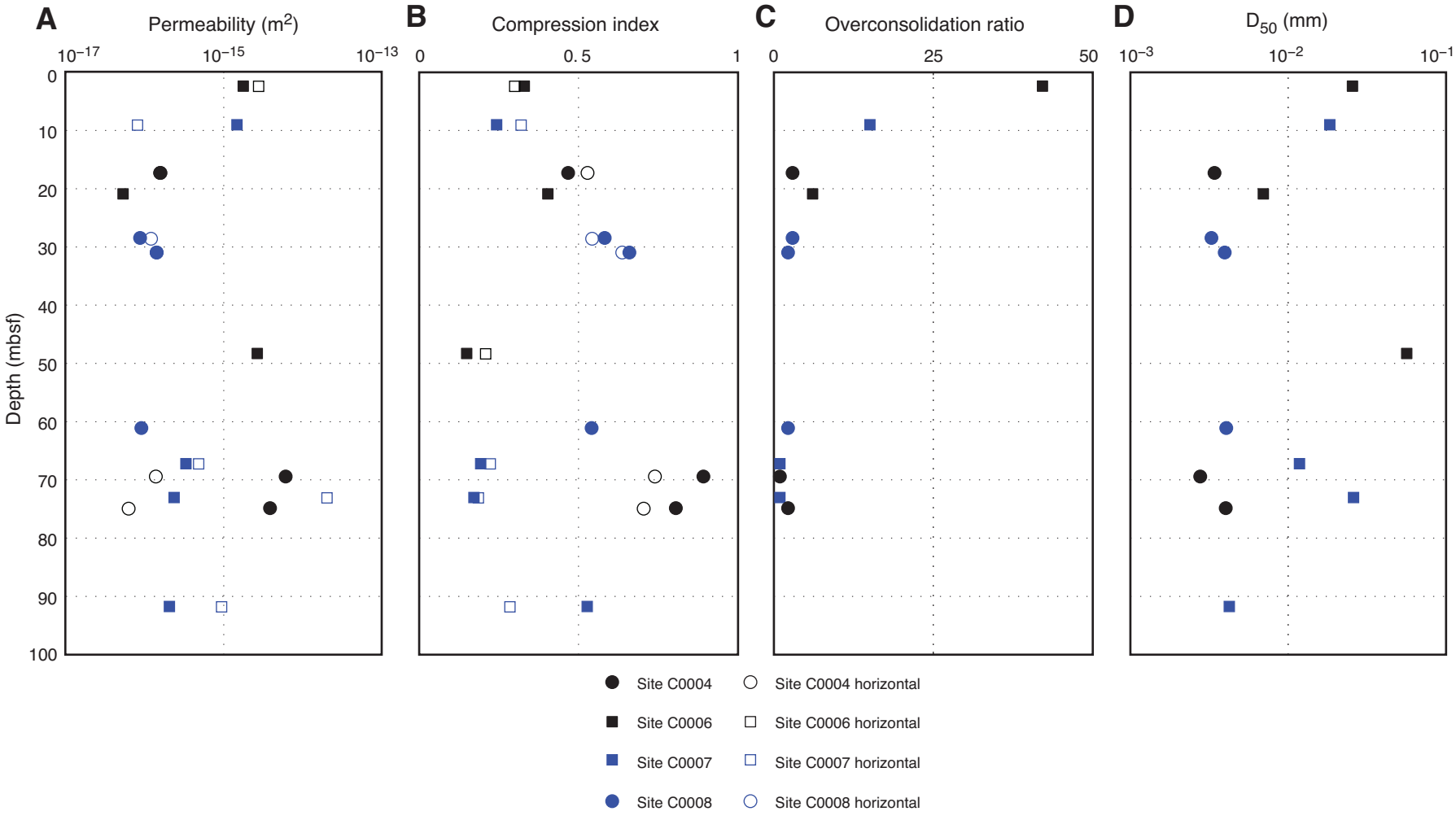

Table T1. Summary of core specimens used in consolidation and grain-size experiments, Expedition 316. (See table note.)

Hole, core, section	Depth (mbsf)	Test number	Core orientation	Experiment
316-				
C0004C-3H-2	17.31	CRS034	Vertical	CRS, grain size
C0004C-7H-9	69.39	CRS035	Vertical	CRS, grain size
C0004C-9H-2	74.86	CRS036	Vertical	CRS, grain size
C0006E-1H-3	2.39	CRS037	Vertical	CRS, grain size
C0006E-3H-6	20.90	CRS038	Vertical	CRS, grain size
C0006E-8H-1	48.31	CRS039	Vertical	CRS, grain size
C0007B-1H-6	9.02	CRS040	Vertical	CRS, grain size
C0007C-7X-5	67.21	CRS041	Vertical	CRS, grain size
C0007C-8X-2	73.03	CRS042	Vertical	CRS, grain size
C0007C-10X-1	91.74	CRS044	Vertical	CRS, grain size
C0008A-4H-6	30.92	CRS045	Vertical	CRS, grain size
C0008C-4H-6	28.52	CRS046	Vertical	CRS, grain size
C0008C-7H-9	61.14	CRS047	Vertical	CRS, grain size
C0004C-3H-2	17.33	CRS048	Horizontal	CRS
C0004C-7H-9	69.42	CRS049	Horizontal	CRS
C0004C-9H-2	74.98	CRS055	Horizontal	CRS
C0006E-1H-3	2.42	CRS056	Horizontal	CRS
C0006E-8H-1	48.36	CRS057	Horizontal	CRS
C0007B-1H-6	9.07	CRS058	Horizontal	CRS
C0007C-7X-5	27.26	CRS059	Horizontal	CRS
C0007C-8X-2	73.08	CRS060	Horizontal	CRS
C0007C-10X-1	91.79	CRS061	Horizontal	CRS
C0008A-4H-6	30.97	CRS062	Horizontal	CRS
C0008C-4H-6	28.57	CRS063	Horizontal	CRS

Note: CRS = constant rate of strain.

Table T2. Example of data from CRS consolidation experiment (portion of CRS036 data) Expedition 316. (See table notes.)

Time (s)	ε (%)	σ_a (kPa)	P_p (kPa)	P_c (kPa)	σ_a' (kPa)	e	K (m/s)	c_v (m^2/s)	Work (kJ/m^3)
0	0.00	26	386	387	26	1.56	NaN	NaN	0.00
240	0.02	37	387	387	36	1.56	NaN	NaN	0.01
480	0.04	43	387	386	42	1.56	NaN	NaN	0.01
720	0.05	48	387	386	47	1.56	NaN	NaN	0.02
960	0.07	49	387	387	48	1.56	NaN	NaN	0.03
1200	0.09	54	387	387	53	1.56	NaN	NaN	0.04
1440	0.10	56	387	386	56	1.56	NaN	NaN	0.04
1680	0.12	61	387	386	60	1.56	1.08E–08	2.31E–05	0.06
1920	0.14	65	387	386	65	1.56	1.11E–08	1.99E–05	0.07
2160	0.15	65	387	387	64	1.56	1.30E–08	2.12E–05	0.08
2400	0.17	68	387	386	68	1.56	1.11E–08	1.78E–05	0.09
2641	0.19	71	387	387	70	1.56	1.33E–08	2.03E–05	0.10
2881	0.20	72	387	387	72	1.55	1.44E–08	1.97E–05	0.11
3121	0.22	77	387	386	77	1.55	1.72E–08	2.23E–05	0.12
3361	0.23	76	387	387	76	1.55	1.53E–08	1.77E–05	0.13
3601	0.25	79	387	387	78	1.55	1.56E–08	1.80E–05	0.15
3841	0.27	80	387	386	80	1.55	1.91E–08	2.20E–05	0.16

Notes: Complete CRS consolidation data for all experiments is in 316_CONSOL in "Supplementary material." All variables are defined in Table T4. NaN = not a number.

Table T3. Bulk physical properties (permeability, compressibility, and grain size) of specimens from Expedition 316. (See table notes.)

Hole, core, section	Depth (mbsf)	Test number	Core orientation	σ_{vh}' (kPa)	σ_{pc}' (kPa)	OCR	$k_{epc'}$ (m^2)	$e_{pc'}$	c_c	e_o	D_{50} (mm)	D_{25} (mm)	D_{75} (mm)	Sand (%)	Silt (%)	Clay (%)
316-																
C0004C-3H-2	17.31	CRS034	Vertical	105	285	2.71	1.6E–16	1.55	0.47	2.7	0.003	0.001	0.019	11	47	42
C0004C-7H-9	69.39	CRS035	Vertical	427	570	1.33	6.1E–15	1.56	0.89	4.1	0.003	0.001	0.011	6	55	40
C0004C-9H-2	74.86	CRS036	Vertical	464	710	1.53	3.8E–15	1.41	0.81	3.7	0.004	0.001	0.014	3	64	33
C0006E-1H-3	2.39	CRS037	Vertical	15	625	41.7	1.8E–15	0.90	0.33	1.8	0.026	0.007	0.058	22	62	16
C0006E-3H-6	20.90	CRS038	Vertical	157	1010	6.43	5.2E–17	0.84	0.40	2.1	0.007	0.002	0.023	5	69	26
C0006E-8H-1	48.31	CRS039	Vertical	395	90	0.228	2.6E–15	0.80	0.15	1.2	0.056	0.031	—	44	50	6
C0007B-1H-6	9.02	CRS040	Vertical	69	1045	15.1	1.5E–15	0.79	0.24	1.5	0.018	0.005	0.050	17	66	17
C0007C-7X-5	67.21	CRS041	Vertical	604	490	0.811	3.4E–16	0.74	0.19	1.3	0.012	0.002	0.030	8	69	24
C0007C-8X-2	73.03	CRS042	Vertical	658	900	1.37	2.4E–16	0.63	0.17	1.2	0.026	0.009	0.058	21	65	14
C0007C-10X-1	91.74	CRS044	Vertical	819	180	0.220	2.1E–16	0.94	0.53	2.2	0.004	0.001	0.013	1	63	36
C0008A-4H-6	30.92	CRS045	Vertical	191	375	1.96	1.4E–16	1.44	0.66	3.2	0.004	0.001	0.010	0	62	38
C0008C-4H-6	28.52	CRS046	Vertical	181	585	3.23	8.8E–17	1.28	0.58	2.9	0.003	0.001	0.009	0	62	38
C0008C-7H-9	61.14	CRS047	Vertical	403	720	1.79	9.3E–17	1.10	0.54	2.7	0.004	0.001	0.015	2	62	36
C0004C-3H-2	17.33	CRS048	Horizontal	105	308	—	1.6E–16	1.51	0.53	2.9	—	—	—	—	—	—
C0004C-7H-9	69.42	CRS049	Horizontal	427	494	—	1.4E–16	1.50	0.74	3.5	—	—	—	—	—	—
C0004C-9H-2	74.98	CRS055	Horizontal	465	679	—	6.7E–17	1.27	0.71	3.3	—	—	—	—	—	—
C0006E-1H-3	2.42	CRS056	Horizontal	15	432	—	2.9E–15	0.92	0.30	1.7	—	—	—	—	—	—
C0006E-8H-1	48.36	CRS057	Horizontal	395	1282	—	—	0.70	0.21	1.4	—	—	—	—	—	—
C0007B-1H-6	9.07	CRS058	Horizontal	69	643	—	8.2E–17	0.83	0.32	1.8	—	—	—	—	—	—
C0007C-7X-5	27.26	CRS059	Horizontal	604	830	—	4.8E–16	0.69	0.22	1.4	—	—	—	—	—	—
C0007C-8X-2	73.08	CRS060	Horizontal	658	1039	—	2.0E–14	0.61	0.19	1.2	—	—	—	—	—	—
C0007C-10X-1	91.79	CRS061	Horizontal	819	1253	—	9.3E–16	0.74	0.28	1.6	—	—	—	—	—	—
C0008A-4H-6	30.97	CRS062	Horizontal	191	285	—	1.4E–16	1.56	0.64	3.2	—	—	—	—	—	—
C0008C-4H-6	28.57	CRS063	Horizontal	181	389	—	1.2E–16	1.29	0.54	2.7	—	—	—	—	—	—

Notes: OCR = overconsolidation ratio. Sand-sized particles are >62.5 µm, silt-sized particles are 2–62.5 µm, and clay-sized particles are <2 µm. All variables are defined in Table T4. — = no data/no analyses.

Table T4. Nomenclature, Expedition 316. (See table note.)

Variable	Definition	Dimension	Unit
c_c	Compression index	Dimensionless	—
c_v	Coefficient of consolidation	L^2/T	m^2/s
D_{25}	Particle size at which 25% are smaller by mass	L	mm
D_{50}	Median grain size	L	mm
D_{75}	Particle size at which 75% are smaller by mass	L	mm
$e_{pc'}$	Void ratio at preconsolidation stress	Dimensionless	—
e_o	Reference void ratio	Dimensionless	—
g	Acceleration due to gravity	L/T^2	m/s^2
H	Instantaneous specimen height	L	cm
H_o	Initial specimen height	L	cm
K	Hydraulic conductivity	L/T	m/s
k	Permeability	L^2	m^2
$k_{e_{pc}'}$	Permeability at in situ void ratio	L^2	m^2
m_v	Coefficient of volume compressibility	LT^2/M	1/kPa
OCR	Overconsolidation ratio	Dimensionless	—
P_p	Pore pressure	M/LT^2	kPa
P_c	Cell pressure	M/LT^2	kPa
ε	Axial strain	Dimensionless	%
$\dot{\varepsilon}$	Strain rate	1/T	1/s
γ_w	Unit weight of water	M/L^2T^2	Pa/m
ρ_b	Bulk density	M/L^3	kg/m^3
ρ_w	Seawater density	M/L^3	kg/m^3
σ_{vh}'	Hydrostatic vertical effective stress	M/LT^2	kPa
σ_a	Total axial stress	M/LT^2	kPa
σ_a'	Axial effective stress	M/LT^2	kPa
σ_{pc}'	Preconsolidation stress	M/LT^2	kPa
σ_{vh}	Hydrostatic effective stress	M/LT^2	kPa
Δ_u	Base excess pressure	M/LT^2	kPa
μ	Dynamic viscosity	M/LT	Pa·s

Note: — = not applicable.